CMT Ceramics in Modern Technologies
TECHNA GROUP srl

Digital Printing of Glass-ceramic Glazes

M. Cannio[a], D.N. Boccaccini[b], R. Taurino[d], V. Riva[c], M.L. Gualtieri[a], M. Tognetti[e], M. Hanuskova[a], M. Cicconi[f], T. Fey[f], M. Rosa[g], V. Novaresio[h], P. Petaccia[h], M. Romagnoli[a], A.R. Boccaccini[i]

[a]Dipartimento di Ingegneria Enzo Ferrari, Università di Modena e Reggio Emilia, Italy; [b]Tecnoitalia S.r.l., Sassuolo - MO, Italy; [c]Metco S.r.l., Fiorano Modenese - MO, Italy; [d]Dipartimento di Ingegneria e Architettura, Università di Parma, Italy; [e]Daxel S.r.l., Rubiera RE, Italy; [f]Institute of Glass and Ceramics, Department of Materials Science and Engineering, University of Erlangen-Nuremberg, Erlangen, Germany; [g]Technical University of Denmark, Department of Energy Conversion and Storage, Roskilde, Denmark; [h]Allovis Engineering Services, Torino, Italy; [i]Institute of Biomaterials, Department of Materials Science and Engineering, University of Erlangen-Nuremberg, Erlangen, Germany

The outstanding versatility shown by Inkjet printing has turned it into a leading technology in several industrial manufacturing fields of which ceramic tile decoration is a good example. Several papers in literature have set the rheological and fluid dynamics characteristic of the inks and the process parameters required for an optimum ink deposition for ceramic tile decoration. However, there is a lack of studies investigating the conditions for the deposition of glass-ceramic glazes. The glazes considered in the present study are intended for digital injection devices using printheads working in the Drop On Demand (DOD) mode based on piezoelectric elements or other digital injection techniques such as continuous ink jet (CIJ), electrovalves, pistons or others. The purpose of this work is to study experimentally the influence of chemical composition and mineralogy acting on the jettability of a range of glass-ceramic glazes. Relevant parameters like viscosity, surface tension and process parameters such as applied pressure, are discussed on the basis of fluid mechanics parameters and printing diagrams. The specific characteristics of digital glaze deposition technologies (continuous jetting and drop on demand) are discussed and the remaining challenges for future applications of the technology are outlined.

Keywords: Glaze Aqueous Inks, Digital Decoration, Ink Stability, Printability Diagram.

1. Introduction

Inkjet printing is a relatively recent technology being increasingly explored for numerous industrial applications [1,2]. In the field of ceramic tile decoration, the use of inkjet printing has grown remarkably in the last ten years to become currently the standard technology in the field [3]. Ceramic tiles are decorated by drop-on-demand (DOD) ink-jet printing, which is the most commonly used technique in modern industrial applications. In a piezoelectric DOD ink-jet printer, upon application of a mechanical pulse from the piezoelectric element, the ink chamber is deformed. Other commercial ink-jet printers exist with different digital injection techniques such as CIJ, or DOD systems based on electrovalves, pistons or other devices [4].

In the ceramic tile manufacturing process, a first glazing step is performed before the ink-jet decoration to provide a white background to the ceramic supports. This glaze is a water based ceramic suspension where the solid content is a mixture of ceramic particles (quartz, kaolin, etc.) and glass-ceramic frits. The glazing process is, however, associated with significant waste of raw materials, high energy requirements and furthermore, contributes to pollution [4]. Glazing is currently carried out by means of a highly unsustainable spraying technology, with losses experimentally demonstrated to be of up to 40% of the glaze due to the nebulization process. This technology further possesses potential health threat to ceramic tile workers as it continuously exposes them to toxic organic binders, fluidising agents and silica (SiO_2) [5]. For example, toxic binders have been linked to acute health conditions like dizziness, nausea, and more serious chronic conditions like leukaemia, scleroderma, renal cancer and toxic encephalopathy (neurological abnormalities) [6]. Furthermore, the use of toxic binders increases the energy required to produce the tiles, as the release of these substances creates a need for suction equipment to remove the vapours from the work place.

Hence research of alternative deposition methods suitable for the tile glazing process has become of outmost importance for its technological implication in the ceramic tile industry and related research institutions.

Digital printing methods, e.g. ink-jet printing, where the deposition area is defined as a function of the tile dimensions, could avoid the waste of glaze as the nebulization process is eliminated. As consequence, no suction cabins are required and this represent a substantial improvement in the working environment. Table 1 shows an overview of the advantages and disadvantages of each glazing technology discussed in the previous paragraphs.

The scope of this work is to study the application of a commercial non-piezoelectric ink-jet printer (DigiGlaze 4.0 ®, Tecnoitalia, Modena, Italy), working with an electromagnetic valve system for the glazing process in tile manufacturing. The impact of chemical composition, mineralogy, particle size distribution, sedimentation rate and agglomeration phenomena of several commercial glazes on stability over time and jettability is studied experimentally.

* *Corresponding author*
E-mail address: maria.cannio@unimore.it

https://doi.org/10.29272/cmt.2019.0010
Received February 28, 2019; Received in revised form May 12, 2019; Accepted May 13, 2019

Table 1. Comparison of the existing glazing technologies.

Main characteristics of the different glazing technologies		
Traditional method	New digital technologies	
Spraying	Drop on demand (DOD) based on piezoelectric valves	Drop on demand (DOD) based on electromechanical dosing system
- Nontoxic-to-contact cheap water based glazes - High pollution of working environment - High waste of glaze - Required suction cabin - High water consumption for cleaning	- Organic solvent based glazes - High pollution of this solvents in the environment on firing - No waste of glaze (area of deposition digitally defined) - No waste of water (no need of suction cabins) - Highly micronized particles for the glaze preparation	- It uses nontoxic-to-contact cheap standard particle size water based glazes - No pollution on firing - No waste of glaze (area of deposition digitally defined) - No waste of water (no need of suction cabins) - No need of further milling

Two different jetting application modes, i.e. CIJ and DOD, are compared in terms of quality of the deposition. Viscosity, surface tension and fluid mechanics parameters are determined for the assessment of printability diagrams in the two different jetting modes and the results are discussed in the context of the peculiarities of digital glaze deposition technology. The best parameters for digital glazing comparing the properties and rheological behaviour of different glazes were found.

2. Experimental

2.1. Materials

Eight different commercial glazes, labelled 554 (DEF Spa, Modena, Italy), EN 48 (Vetriceramici-Ferro Spa, Modena, Italy), 3293 (Vetriceramici-Ferro Spa, Modena, Italy), SL711 (Vetriceramici-Ferro Spa, Modena, Italy), M490 (Ferro Corp., Cleveland, Ohio, USA), 277B (Ferro Corp., Cleveland, Ohio, USA), 277A (Ferro Corp., Cleveland, Ohio, USA), used by the ceramic tile manufacturing industry from Sassuolo area, (Italy), were thoroughly characterized in terms of chemical and mineralogical composition, rheological behaviour, stability, acid-basicity, surface tension and contact angle properties. The glazes were taken directly from the ceramic tile companies who collaborated in this work after the milling process. The densities were in the 1600-1700 g/L range. The additives in the glazes at this stage (after milling) are just those used to help the evacuation of the glazes from the mills.

2.2. Additivation/preparation of glazes for digital printing

The glazes were standard water based suspensions typically used by spraying technology with additives provided by Daxel S.r.l (Rubiera, Italy), which are specially studied and prepared for this ink-jet application. Suspension stability, constancy of rheological parameters and good wetting properties are desirable for any type of glaze. These properties become particularly essential when the glazes must flow in the circuit of a digital machine, where they experience major mechanical stresses derived from sudden accelerations and stops at very high frequency. The investigated additive called A164® (Daxel S.r.l., Italy) is a mix of different components for the achievement of these goals.

Glaze preparation for digital printing

Glazes were prepared with various amounts of additive (0, 5 and 10 wt%) to analyse its influence on rheological properties and surface tension. The additive was mixed with the glaze for 30 min in an industrial stirrer and the suspension was then passed through a 10800 mesh (53 microns) (270 ASTM mesh) sieve. Formulations with the same amount of additive (5 or 10 wt%) but with different densities (1240, 1360, 1510 g/L) were also prepared to investigate the influence of density on printing quality. The corresponding solid fractions for the densities of (1240, 1360, 1510) g/L are (29.03, 39.71, 50.66) wt%.

2.3. Characterization of glazes

XRD and quantitative analysis

The dried glazes were characterized by X-ray Powder Diffraction (XRPD) using a θ/θ diffractometer equipped with a real time multiple strip (RTMS) detector (PANAlytical, X'Pert PRO diffractometer, Almelo, The Netherlands). The XRD patterns were collected in the angular region from 3° to 80° 2θ at room temperature. A Ni filter, divergence and anti-scattering slits (0.25°), and a soller slit (0.04 rad) were mounted in the incident beam pathway. A virtual step scan having a step-size of 0.0167° 2θ was used. All powders were mounted on a flat Al-holder by side-loading in order to minimize preferred orientation of the crystals. Rietveld refinements were accomplished using the General Structure Analysis System [7,8] in conjunction with its graphical interface EXPGUI [9,10], giving quantitative data on the phase composition. Silicon NIST® SRM® 640e in powder was used as internal standard, as suggested in ref. [11].

Chemical characterization

X-ray fluorescence quantitative chemical analyses (XRF, ARL ADVANT'XP+ X-ray fluorescence sequential spectrometer, Thermo Scientific, Waltham, MA) were performed on the glazes. The results were converted in the form of the most stable oxides.

Contact angle and surface tension

Static angle measurements of the slurries on the ceramic substrate were carried out with the "Sessile drop" method using the DataPhysics OCA 20 instrument.

Measurements were performed using a drop volume of 3 μl and the SNS-D051 / 025 needle with a diameter of 0.52 mm. 10 measurements per sample were performed. The surface tension of the slips was obtained with the "Pendant drop" method, using a SND-091/061 needle with a diameter of 0.91 mm. 10 measurements per sample were performed.

Rheological characterization

A Haake Rheostress (RS-1) rheometer equipped with a Z34DIN Ti sensor was used to record rheological data in the controlled shear rate mode (CR). The procedure used for these measurements is summarized as follows. The temperature was controlled and kept at 25 °C by means of an external thermostat connected to the rheometer. The steps used to record the flow curve are the following: 1) CR 300 s^{-1}, Time: 30 s, 2) CR 0 s^{-1}, Time: 60 s, 3) CR from 0 to 300/2500s^{-1}, Time: 300 s, 4) CR from 300/2500s^{-1} to 0, Time: 300 s.

2.4. Digital printing

The glazes were deposited by means of an industrial ink-jet printer (Digiglaze 4.0®) provided by Tecnoitalia S.r.l. (Modena, Italy), which uses a non-piezoelectric electro-mechanical drop dispenser system, giving the possibility to work in both CIJ and DOD modes with water based glazes. The flow rate (g/s) can be controlled by changing the feeding pressure, the line speed and the diameter of the nozzles. The main characteristics of the printer used are listed below:

- Nozzle step in the transversal direction: 2.1 mm
- Manufacturing line speed: 0-50 m/min
- Nozzle diameter: 250-600 μm
- Feeding pressure: 0-1.5 bar
- Drop frequency: 0-600 Hz

In this study, the glazes were printed onto substrates, pre-heated at 100 °C, of the same porcelain stoneware tile composition. The samples were prepared with the same weight per square meter (441g/m^2) for the study of the tile aesthetics and definition of the Quality deposition parameter (QDP). Then the tiles were fired following the standard fast firing cycle of industrial roller furnaces. The velocity of the line was kept constant at 30 m/min, which is a typical value used in the ceramic tile industry. In order to compare the influence of pressure on the quality of deposition, the velocity of the manufacturing line was kept constant and the pressure was increased. Table 2 reports the variation of the weight of glaze applied by square meter as function of the feeding pressure for a printhead with a nozzle step of 2.1 mm, nozzle orifice of 500 μm and a line velocity of 30 m/min. The tests in DOD mode were performed at a frequency of 200 Hz.

2.5. Characterization of the printed layers

SEM- EDS and Light microscopy analyses of fired tile samples

The microstructure of fired tile samples, both in plane and in cross section, was characterized using a SEM (ZEISS Auriga base) equipped with an EDS detector (Oxford Instruments 80 mm^2 solid state drift detector). For these observations, small pieces of tile samples were mounted uncoated on an aluminium stub with conductive adhesive Cu band.

Light microscopy imaging of the polished cross-section of a tile glazed with 277B was performed using a Olympus GX51 instrument with SC30 Olympus optics. The thickness (determined by image analyses using the freeware ImageJ) as a function of distance from the short side of the tile (perpendicular to the traveling direction) was determined.

3. Results

3.1. Characterization of glazes

XRD and quantitative Rietveld analysis

Table 3 reports the quantitative phase analysis results obtained by XRPD and Rietveld refinement. The glazes labelled 277A, 277B,

Table 2. Variation of the weight of glaze as function of the applied pressure in CIJ jetting mode.

Feeding pressure in CIJ mode (bar)	Feeding pressure in DOD mode (bar)	Flow rate by nozzle (g/sec)	Glaze weight (g/m^2)
0.9	0.5	0.42	342
1	0.6	0.46	375
1.1	0.7	0.51	412
1.2	0.8	0.54	441
1.3	0.9	0.57	465
1.4	1	0.61	494

Table 3. a) Data from XRD analysis and quantitative Rietveld refinement (wt%).

Data from quantitative Rietveld refinement (wt%)										
Sample	Quartz	Illite	Zircon	Kaolin	Alumina	Albite	Dolomite	Wollastonite	Amorphous	Crystalline: amorphous ratio
554	13.6	3.27	18.75	13.18		25.42	0.51		25.26	2.96
EN 48	22.91	6.14	9.76	22.79		11.38			26.99	2.70
3293	21.56	5.78	15.48	21.45		10.71			25.40	2.95
SL711	20.21	5.51	9.85	14.7		10.06	1.44		38.19	1.62
M490	34.37	5.9	11.27	4.44	9.13	1.33			33.54	1.98
277B	40.97	5.27	12.94	4.27					36.54	1.74
277A	27.55		10.65	3.55	12.87			0.96	44.38	1.25

b) Reference of the starting structure model for the refinement.

Phase	Chemical Formula	Reference
Quartz	SiO_2	Prewitt et al., 1976[12]
Muscovite Illite	$K_2Al_4(Si_6Al_2O_20)(OH)_4$ $K_{0,65}Al_{2,0}[Al_{0,65}Si_{3,35}O_{10}](OH)_2$	Guggenheim et al., 1987[13] Collins & Catlow 1992[14]
Zircon	$ZrSiO_4$	BA Kolesov et al., 2001[15]
Kaolin	$Al_2Si_2O_5(OH)_4$	Bish D L, Von Dreele R B. 1932[16]
Alumina	Al_2O_3	Lewis et al.,1989[17]
Albite	$NaAlSi_3O_8$	Phillips et al. 1971[18]
Dolomite	$Mg,Ca(CO_3)_2$	Steinfink & Sans 1959[19]
Wollastonite	$CaSiO_3$	Mamedov & Belov 1956[20]

Table 4. Chemical composition obtained from XRF analyses.

Chemical analysis (wt%)						
Sample	Na_2O	Al_2O_3	SiO_2	K_2O	CaO	ZrO_2
554	3.06	17.74	57.62	1.4		20.18
EN 48	4.05	21.79	63.63	2.2		8.34
3293	3.07	20.97	51.73	1.76		22.47
SL711	3.35	21.93	60.2	2.31		12.21
M490	2.16	11.53	67.19	1.42	5.4	12.3
277B	2.42	13.49	63.6	1.5	5.67	13.32
277A		18.53	59.65	1.61	5.54	14.67

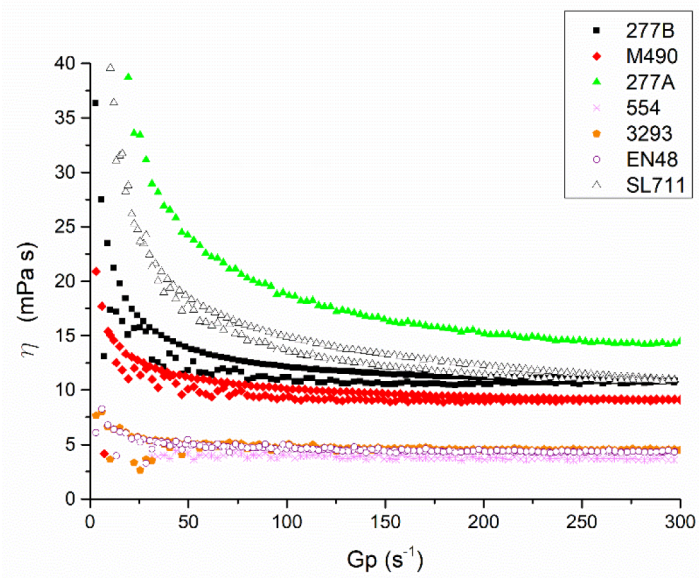

Figure 1. Viscosity as function of the shear rate for all the investigated glazes in as-received state (without additive addition).

SL711 and M490 have the highest amount of amorphous phase which is due to a higher frit content of these glazes.

Chemical characterization

Table 4 reports the chemical composition obtained from XRF analyses.

Samples 554 and 3293 have the highest content of ZrO_2, while sample M490, EN48 and 277B show highest values of SiO_2. In sample EN48, 3293 and SL711 there is a high amount of Al_2O_3. Samples M490, 277B and 277A show the presence of CaO at the average concentration of 5.5 wt %.

Rheological characterization

The flow curves in Figure 1 show the viscosity as function of shear rate for all the investigated glazes in the as-received state (without additive). 277A, SL711, 277B and M490 are the compositions characterized by the highest values of viscosity, while EN48, 3293 and 554 show the lowest viscosity values.

Figure 2a) and 2b) show the variation of viscosity at high values of Gp (2500 s^{-1}) for the additive concentrations of a) 5 wt% and b) 10 wt%, respectively.

Contact angle and surface tension

Table 5 shows the results from contact angle measurements obtained from sessile and pendant method for the investigated glazes at density of 1360 g/L without additive and with 10 wt% of A164 addition.

Table 5 also reports the values of surface tension for all the glazes at density of 1360 g/L and with 0 wt%, 5 wt% and 10 wt% of A164 additive, measured by Force Tensiometer.

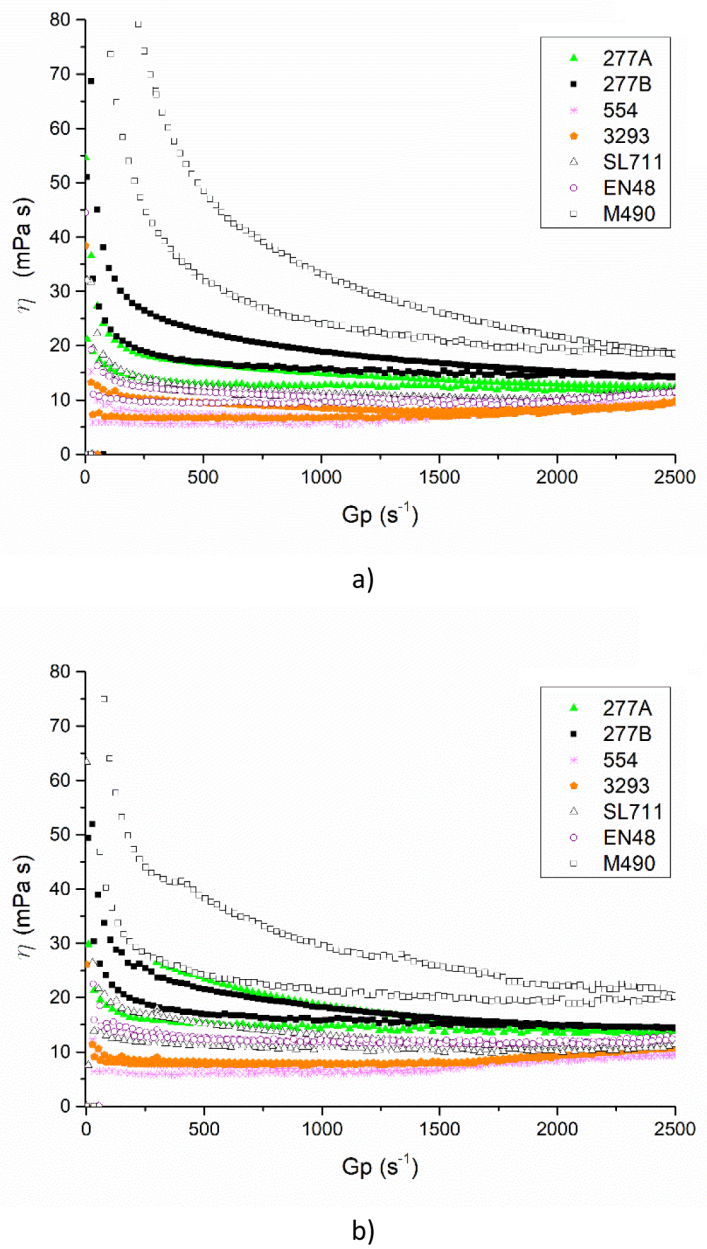

Figure 2. Influence of additive concentration at high values of Gp for a) 5 wt% and b) 10 wt% of additive concentration.

3.2. Characterization of printed samples

Light microscopy of fired tiles

Figure 3 shows the results obtained from light microscopy observations on top plane view of fired tile samples. In particular, in some samples, e.g. 277A and 277B, it is possible to note the formation of defect lines which are clearly evident in the direction of advancement of the manufacturing line perpendicular to the printhead. The presence of these linear ripples is more evident with glazes at high viscosity and when the method of deposition employed was continuous jetting (CIJ).

Light microscopy images in cross-section were also acquired and processed by image analysis for the characterization of the morphology of the defects. A complete tile side of sample 277B was pictured and the thickness was characterized by image analysis for the determination of the variation in thickness. The variation of the tile thickness along the complete tile side is shown in Figure 4.

It was found that this variation in glaze thicknesses corresponds with the linear ripples observed on the tile surface, i.e. higher thickness corresponds to the ripple peaks while lower thickness corresponds to the ripple channels.

Table 5. Static contact angle (θs) and surface tension (γ) of as received and additivated glazes at density of 1360 g/L obtained from both sessile, pendant drop and force tensiometer methods.

Sample	θs (°) Sessile, pendant drop method No additive	θs (°) Sessile, pendant drop method 10 wt% A164	γ (mN/m) No additive Force Tensiometer	γ (mN/m) 5 wt% A164 Force Tensiometer	γ (mN/m) 10 wt% A164 Force Tensiometer
554	26.2±5.1	43.9±2.3	69.1	40.0	36.0
EN48	41.3±3.2	53.9±1.1	72.3	44.0	35.0
3293	30.2±5.2	34.2±2.2	71.2	46.3	36.0
SL711	45.8±0.2	45.85±0.2	62.0	41.0	36.0
M490	74.8±3.1	56.2±2.7	66.1	68.0	52.0
277B	51.2±4.3	n.m	65.2	45.0	46.0
277A	42.1±5.6	n.m	66.5	44.0	43.0

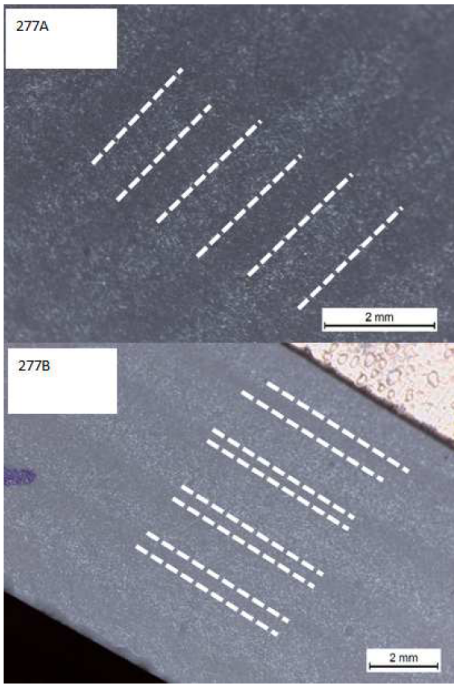

Figure 3. Top-view light microscopy images of samples 277A and 277B. The arrows indicate the light and dark lines observed on the tile surface.

SEM and EDS analysis

Analysis of defects in plane view

In the case of deposition of glazes at low viscosity and/or density values in CIJ mode, the presence of defects characterized by a pattern of glossy and matte lines along the tile was found. In this case, SEM and EDS in plane view images were used to investigate if these lines may be produced because of a separation between the amorphous and crystalline phases present in the glazes. A 277B sample tile deposited with a glaze in conditions of very low density (1250 g/L) and viscosity (5 mPa s) was selected to perform this investigation. Figure 5 shows top-view SEM images of a piece of this 277B tile performed on the surface of the defects on both matte (left) and glossy areas (right). Figure 6 reports the results of the EDS analysis performed in these areas. No significant difference in chemical composition was observed.

4. Discussion

4.1. Digital printing

As mention previously, two clear types of defects were observed on fired tiles depending on the viscosity of the glazes, as shown in the pictures and designs of Figure 7 corresponding to 277B tiles. In particular, for glazes with densities > 1380-1400 g/L, linear ripples were observed along the tile in the same direction of the tile advancement in the manufacturing line. However, when

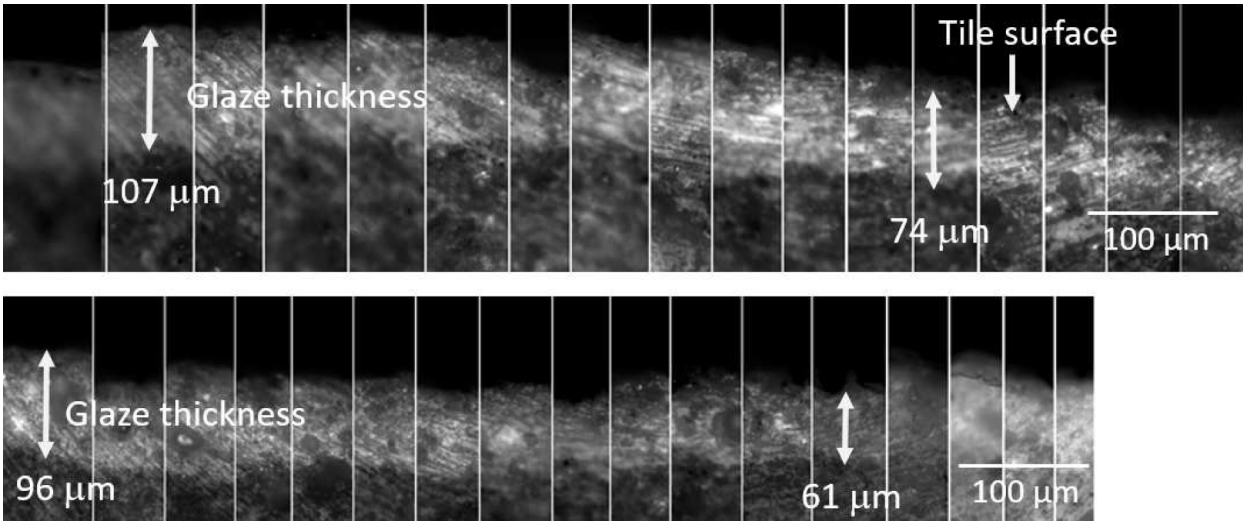

Figure 4. Light microscopy cross-section images of the glaze (polished) along the tile side, showing a large variation in thickness.

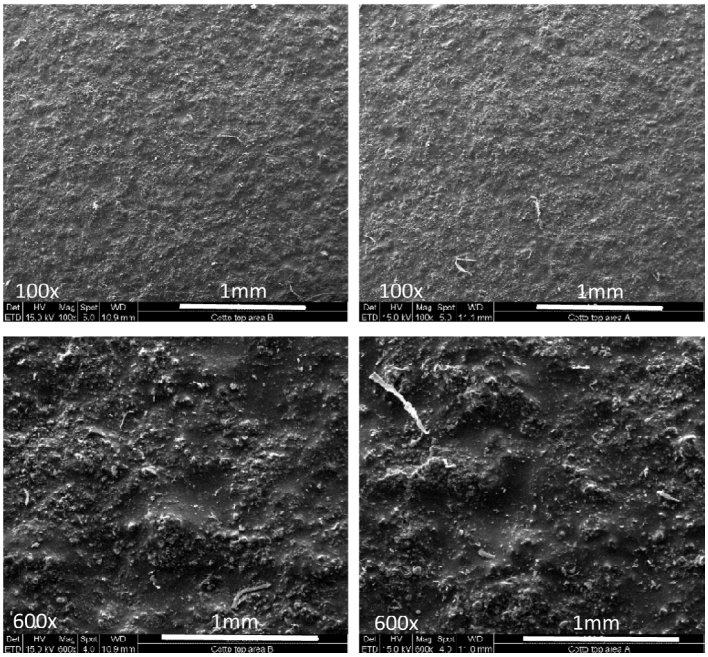

Figure 5. Top-view SEM images of the tile surface on both glossy areas (left) and matte areas (right).

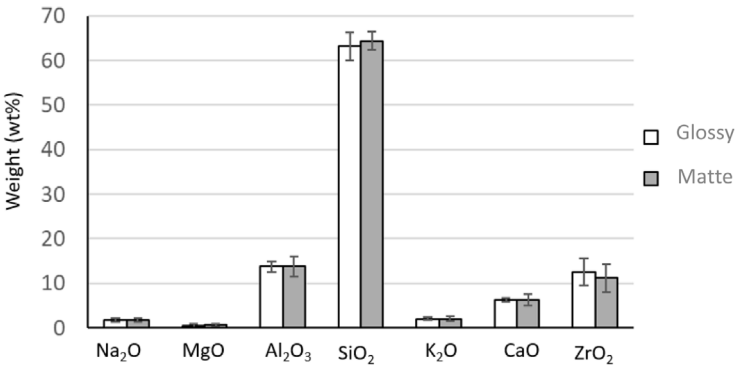

Figure 6. EDS analysis results from glossy and matte areas. No difference in chemical composition was observed.

the density is lower than 1300-1320 g/L a pattern of matte and glossy lines becomes clearly observable on the surface of the tile. It is worth highlighting that these defects were appreciable when the printer was set on CIJ mode, while in DOD mode they were not significant in any the investigated glazes.

The results of the deposition were quantified by the definition of a quality of deposition parameter (QDP). This parameter was defined in collaboration with the ceramic tile industries that own the glazes used in this investigation and from the qualitative analysis carried out by industrial experts in the characterization of the aesthetic properties of the tiles. The objective factor consider here is the aesthetics quality of the final fired products, which was performed by professionals working in the ceramic tile companies who collaborate in this project, by detailed visual observations. Ten different tile samples by glaze composition printed under the same conditions, i.e. glaze weight, velocity of line and feeding pressure, were used to define the QDP parameter. The selected tiles for the definition of the QDP parameter were obtained from glazes with 10 wt% of A164 additive addition. Table 6 reports the results of these analyses which highlight that all glazes show excellent printability when the printer is set in the DOD mode, while the quality of printing is lower in some glazes (e.g. SL711, M490, 277/B and 277/A) when they are printed in CIJ mode.

4.2. Influence of physical-chemical, mineralogical, rheological properties on quality of printing

The glazes were characterized in detail in order to analyse which of their mineralogical, physical-chemical or rheological properties influences the quality of deposition to a greater degree. Based on the mineralogical characteristics of the glazes reported in Table 3, the relation between the amount of crystalline and amorphous phase has been elaborated and reported in Table 3. From this Table, comparing the crystalline to amorphous ratio with the quality parameter, it is evident that glazes with a higher amount of amorphous phase are more challenging to print than glazes with higher crystalline content, particularly in CIJ mode, this being a very important finding of the present study, for its practical and

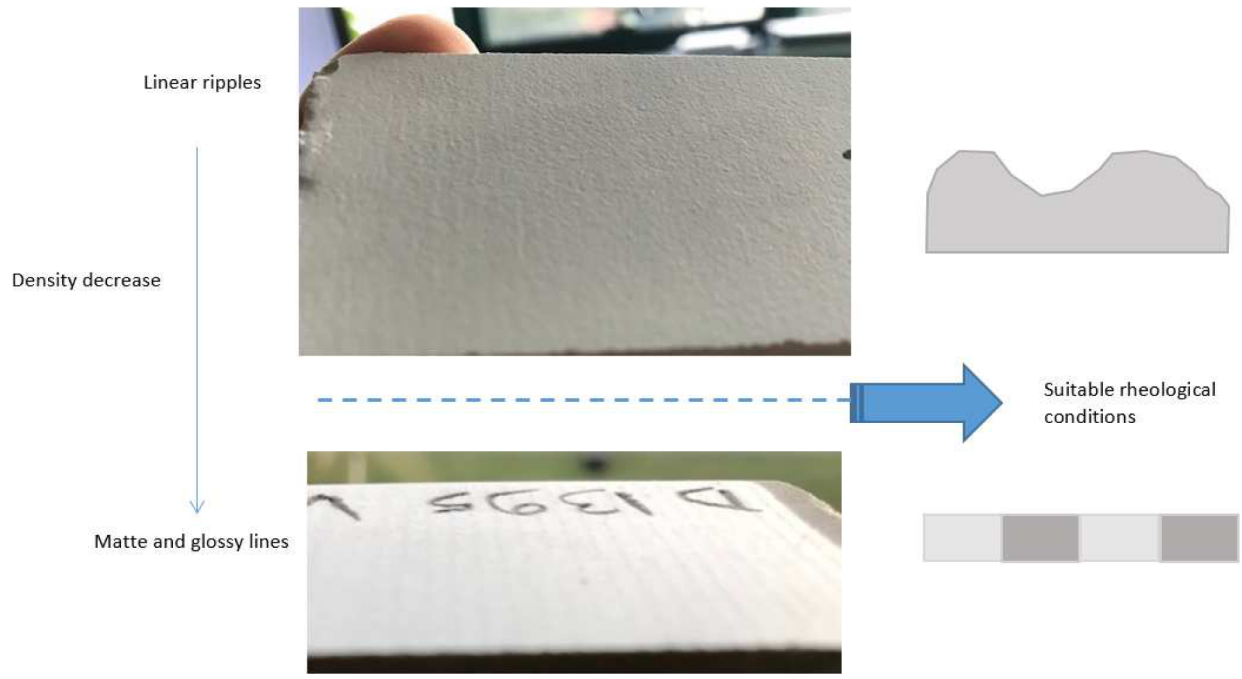

Figure 7. Defects observable on the surface of a 277B tile sample: linear ripples at high densities an alternative glossy/matte pattern at low densities.

Table 6. Quality of deposition of the final products (fired) as defined by the quality of deposition parameter (QDP) obtained by optical observations from industrial experts in tile aesthetics from the tiles companies owning the glazes used in this investigation.

Sample	Quality deposition parameter (QDP) CIJ mode	Quality deposition parameter (QDP) DOD mode
	From 0-10 (10 excellent; <5 low performance)	
554	10	10
EN48	9	10
3293	8	10
SL 711	6	9
M490	5	9
277B	4	9
277A	4	9

industrial relevance.

Taking into consideration the chemical analysis of the investigated glazes, M490 and both 277A and B have the highest CaO concentration (see Table 4). As known, Ca, usually used as a network modifier, influences the solubility of some oxides and other alkaline elements present in glazes and other glassy systems [21,22]. This process eventually may lead to a disconnectivity in the glass network resulting in the formation of silanol groups. Ca reacts with Si, Al and alkaline elements such as Na present in the glaze likely leading to a localized formation of stripes and defects (due to the concentration of alkali and calcium compound) when water evaporates. Furthermore M490 and both 277A and B show the highest values of viscosity, which affects the printing behaviour especially when the CIJ method is used. In fact, the printability region is reduced if compared with DOD method because these glazes with high CaO content exhibit some difficulties in spreading at high viscosity values (linear ripples) while at low viscosity a local separation of frits from the amorphous phase occurs.

The influence of the rheological characteristic of the glazes on the quality of deposition was studied by analysing the effects of density, viscosity and surface tension. Figure 1 shows the variation of viscosity as function of the shear rate for all the investigated glazes without additive addition, while Figure 2 indicates the influence of additive addition on viscosity. All samples in Figure 1 show a shear thinning behaviour. A low hysteresis between the up and down curves is indicative of low time-dependency. The samples shown in Figure 2 maintain a shear thinning or Newtonian behaviour. However, the addition of the additives increases in some cases (e.g. 277A, B and M490) the hysteresis between the up and low curves, probably due to an increase of the time-dependency. This trend is often due to the establishment of weak bonding among the solid particles. It is evident from this figure that the higher is the percent of additive addition, the higher is the increase in viscosity. The addition of the additive, in some samples, produces the onset of a dilatancy at higher shear rates. It is important to note that the values tend to stabilize after (300-500) s^{-1} for almost all the glazes, excluding the compositions 277A, 277B and M490. Considering that the velocity of the glaze in the nozzle orifice is in the range 4-8 m/s for feeding pressures in the range of 0.6-1 bar, viscosity values measured at (300-500) s^{-1} of shear rate correspond to values of tangential velocity of 4-8 m/s that are in the same range of the glaze velocity in the outlet of the nozzles.

Table 7 shows the variation of surface tension and viscosity as function of the additive addition. To achieve a good quality of deposition, the additive must guarantee stable viscosity values in the range of velocities corresponding to the jet or drop ejection from the nozzle while decreasing the surface tension values once deposed on the substrate. For a better understanding of the role of the rheological properties of the glazes and the interaction with the process parameters of the printer, the generated printing diagrams are reported and discussed in the next section.

4.3. Design of printability fluid region in CIJ mode

To analyse the interaction between process parameters and the rheological behaviour of glazes, the printing diagram of the Digiglaze 4.0 printer was built. The details of the construction of these useful diagrams are discussed in literature [23]. Briefly, based on semi-empirical models obtained from experience and related with the occurrence of the main phenomena involved in ink-jet printing (drop formation, possible presence of satellite drops and drop splashing during impact), a printable fluid region of reference has been individuated for the printer used in this investigation for both operating modes, CIJ and DOD [23]. The printable fluid region is defined in a diagram in the space generated by a range of values of the two most representative dimensionless numbers for such phenomenon, namely the Reynolds and Ohnesorge numbers [4][23]. The Reynolds (Re) number is the ratio of inertial to viscous forces (Equation 1), while the Ohnesorge number (Oh) (Equation 2) compares the viscous forces with the capillary and inertial ones. The equations to calculate these numbers are:

$$Re = \frac{\rho\, v\, d}{\eta} \qquad \text{Equation 1}$$

$$Oh = \frac{\eta}{\sqrt{\rho\, \gamma\, d}} \qquad \text{Equation 2}$$

where ρ, υ, d, η, γ are the density, droplet velocity, nozzle

Table 7. Summary of all measured properties of glazes, required for the calculation of the fluid dynamic numbers and for the application points in the printability diagram.

Glaze	Density (ρ)	Surface tension No additive	Viscosity at 285 s^{-1} No additive	Surface tension 5 wt% A164	Viscosity at 285 s^{-1} 5 wt% A164	Surface tension 10 wt% A164	Viscosity at 285 s^{-1} 10 wt% A164
Units	(kg/m^3)	(mN/m)	(mPa. s)	(mN/m)	(mPa. s)	(mN/m)	(mPa. s)
554	1.36	69.00	3.67	40.00	5.22	36.00	8.47
EN48	1.36	72.00	4.34	44.00	12.22	35.00	12.36
3293	1.36	71.00	4.62	46.30	6.30	36.00	10.35
SL 711	1.36	62.00	11.07	41.00	11.44	36.00	13.42
M490	1.36	66.00	9.18	68.00	33.38	52.00	30.28
277B	1.36	65.00	10.87	45.00	22.98	46.00	25.39
277A	1.36	66.00	14.57	44.00	15.44	43.00	24.00

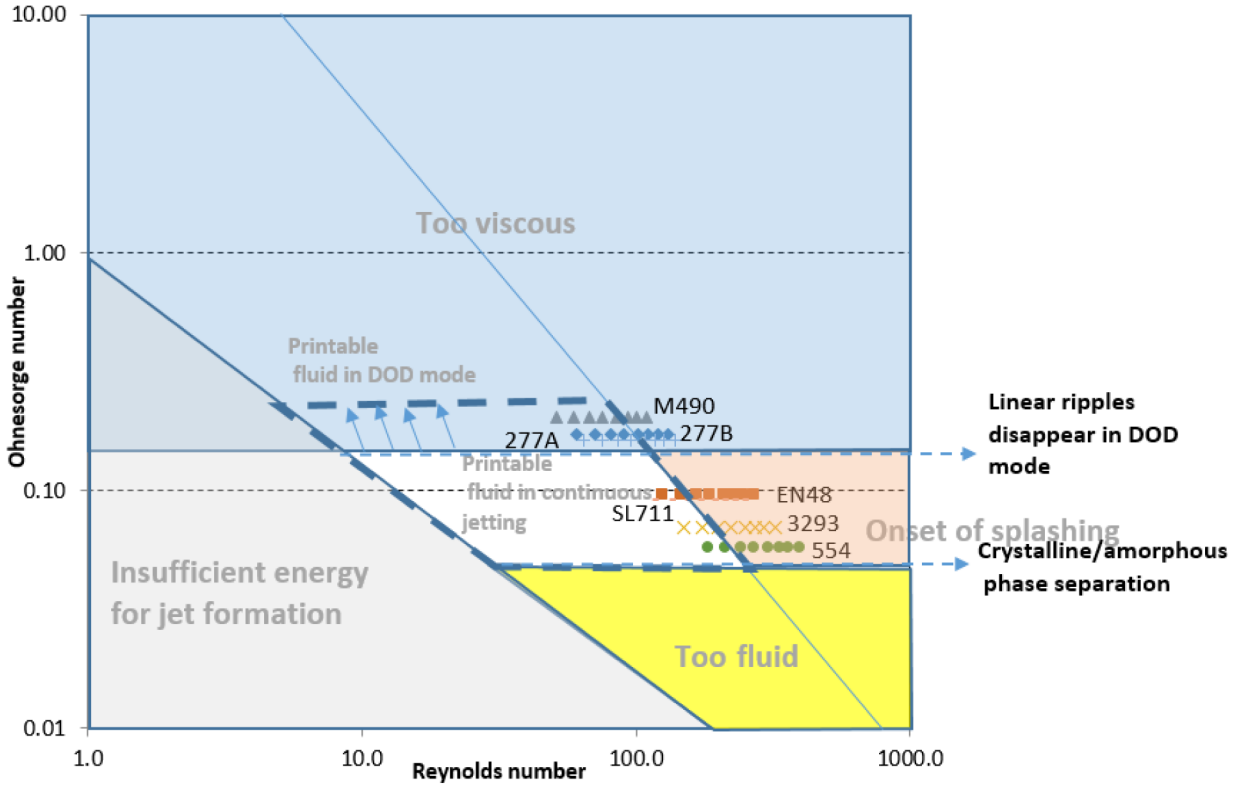

Figure 8. Comparison between DOD and CIJ mode printable fluid zones. All the investigated glazes have been positioned into the diagram for the density of 1360 g/L and additive content of 10 wt%.

diameter, viscosity and surface tension, respectively.
Table 7 summarizes all the measured properties of the glazes required for the calculation of the fluid dynamic numbers and hence for the application points in the printability diagram.

4.4. Design of printability fluid region in CIJ vs. DOD mode

Finally, Figure 8 plots a comparison between DOD and CIJ mode printable fluid zones. All the investigated glazes have been positioned into the diagram for the density values of 1360 g/L and additive content of 10 wt%. It is possible to observe that decreasing the feeding pressure a positive effect on printability is achieved, moving the application point to the left side in the diagram, towards the printability region. This figure also confirms the higher dimension of the printability zone for the DOD mode, giving rise to the possibility to print critical glazes, such as 277A, 277B and M490, which are unprintable in CIJ mode (see Table 6). The critical aspects of these glazes are related to their high surface tension values despite the additive content of up to 10 wt%, the high values of viscosity and the application mode. Depositing a line of material by continuous jetting onto a substrate is challenging when the surface tension is high. On the other hand, DOD mode permits to print small drops than can be controlled in size and frequency, resulting in a better homogenization of the glaze deposition: i.e. in DOD mode, the linear ripple defects disappear.

5. Conclusions

In this work, the application of ceramic glazes by using digital printing is presented for the first time. The glazes were characterized in detail to study the influence of their properties on the quality of the deposition. Two different printing methods were used, CIJ and DOD mode, to compare their respective advantages and disadvantages. Two kind of defects were found depending on the viscosity of the glazes. In CIJ mode at high glaze viscosity linear ripples appear along the tile in the direction of advancement of the manufacturing line. This defect could be due to the lack of spreading of the line of glaze deposited on the substrate because of the high viscosity. On the other hand, at low viscosities, glossy and matte lines appears, also in the direction of tile advancement in the manufacturing line. This later defect could be due to the separation between the amorphous and crystalline phases constituting the glazes. It was also found that the higher is the percentage of frit and Ca in the glaze, the higher is the possibility of this defect to occur. In the case of deposition with the printer in DOD mode, no significant defects were found for all the investigated glazes and a high quality of deposition was achieved.
It was found that surface tension and viscosity are the main properties of the glazes influencing the quality of the printed layers. The higher is the increase in viscosity and the lower is the surface tension achieved through the additivation of the glazes, the better is the quality of deposition.
Process parameters such as step between the nozzles and feeding pressure play also a key role affecting the quality of the printed product. In this work, the step between nozzles was kept constant but the influence of the glaze feeding pressure was investigated. It was found that low pressure leads to higher quality of the deposited glaze layers. In particular, when the CIJ mode is used, low viscous glazes improve the spreading of the glazes and with low feeding pressure it is possible to avoid the occurrence of the glossy-matte lines.
Finally, the use of printing diagrams proved to be a valid tool for the preparation of glazes to be used in digital printing, both from a rheological point of view and from the point of view of the process parameters to be used. It could be determined how the feeding pressure, additive concentration, density and hence the viscosity and surface tension influence the deposition, and how is possible, by changing these parameters, to move from a point which is outside the printability region to the region of printable fluids.

Acknowledgements

The authors would like to thank Prof. Cristina Siligardi (Dipartimento di Ingegneria Enzo Ferrari, Università di Modena e Reggio Emilia) and Prof. Federica Bondioli (Dipartimento di Ingegneria e Architettura, Università di Parma) for helpful discussions about materials for digital printing process.

References

[1] D. Jang, D. Kim, J. Moon, Influence of fluid physical properties on ink-jet printability, Langmuir. (2009). doi:10.1021/la900059m.

[2] B. Derby, Inkjet printing ceramics: From drops to solid, J. Eur. Ceram. Soc. (2011). doi:10.1016/j.jeurceramsoc.2011.01.016.

[3] M. Dondi, M. Blosi, D. Gardini, C. Zanelli, Ceramic pigments for digital decoration inks: An overview, CFI Ceram. Forum Int. (2012).

[4] G.L. Güngör, A. Kara, D. Gardini, M. Blosi, M. Dondi, C. Zanelli, Ink-jet printability of aqueous ceramic inks for digital decoration of ceramic tiles, Dye. Pigment. (2016). doi:10.1016/j.dyepig.2015.12.018.

[5] C.M. Liao, B.C. Wu, Y.H. Cheng, S.H. You, Y.J. Lin, N.H. Hsieh, Ceramics manufacturing contributes to ambient silica air pollution and burden of lung disease, Environ. Sci. Pollut. Res. (2015). doi:10.1007/s11356-015-4701-6.

[6] P. Duch, A.W. Norgaard, J.S. Hansen, J.B. Sorli, P. Jacobsen, F. Lynggard, M. Levin, G.D. Nielsen, P. Wolkoff, N.E. Ebbehoj, S.T. Larsen, Pulmonary toxicity following exposure to a tile coating product containing alkylsiloxanes. A clinical and toxicological evaluation, Clin. Toxicol. (2014). doi:10.3109/15563650.2014.915412.

[7] R. Von Dreele, A. Larson, General structure analysis system (GSAS), Los Alamos Natl. Lab. Rep. LAUR. (2000). doi:10.1103/PhysRevLett.101.107006.

[8] A.F. Gualtieri, V. Riva, A. Bresciani, S. Maretti, M. Tamburini, A. Viani, Accuracy in quantitative phase analysis of mixtures with large amorphous contents. the case of stoneware ceramics and bricks, J. Appl. Crystallogr. (2014). doi:10.1107/S160057671400627X.

[9] B.H. Toby, EXPGUI, a graphical user interface for GSAS, J. Appl. Crystallogr. (2001). doi:10.1107/S0021889801002242.

[10] B.H. Toby, R.B. Von Dreele, GSAS-II : the genesis of a modern open-source all purpose crystallography software package, J. Appl. Crystallogr. (2013). doi:10.1107/s0021889813003531.

[11] A.F. Gualtieri, Accuracy of XRPD QPA using the combined Rietveld-RIR method, J. Appl. Crystallogr. (2000). doi:10.1107/S002188989901643X.

[12] C. Prewitt, S. Sueno, J. Papike, The crystal structures of high albite and monalbite at high temperatures, Am. Mineral. 61 (1976). http://ammin.geoscienceworld.org/content/61/11-12/1213.short.

[13] S. Guggenheim, Y.-H. Chang, A.F.K. van Groos, Muscovite dehydroxylation : studies, Am. Mineral. 72 (1987) 537–550.

[14] D.R. Collins, C.R.A. Catlow, Computer simulation of structures and cohesive properties of micas, Am. Mineral. (1992).

[15] B.A. Kolesov, C.A. Geiger, T. Armbruster, The dynamic properties of zircon studied by single-crystal X-ray diffraction and Raman spectroscopy, Eur. J. Mineral. 13 (2001) 939–948. doi:10.1127/0935-1221/2001/0013-0939.

[16] D.L. Bish, R.B. Von Dreele, Rietveld Refinement of Non-Hydrogen Atomic Positions in Kaolinite, Clays Clay Miner. (1989). doi:10.1346/CCMN.1989.0370401.

[17] J. Lewis, D. Schwarzenbach, H.D. Flack, IUCr, Electric field gradients and charge density in corundum, α-Al_2O_3, Acta Crystallogr. Sect. A. (1982). doi:10.1107/S0567739482001478.

[18] M.W. Phillips, A.A. Colville, P.H. Ribbe, The crystal structures of two oligoclases: A comparison with low and high albite, Zeitschrift Fur Krist. - New Cryst. Struct. (1971). doi:10.1524/zkri.1971.133.133.43.

[19] H. Steinfink, F.J. Sans, Refinement of the Crystal Structure of Dolomite, Am. Mineral. 44 (1959) 679-682. http://scripts.iucr.org/cgi-bin/paper?S0909049595099389.

[20] B.N. V Mamedov K S, The crystal structure of wollastonite, Dokl. Akad. Nauk SSSR. 107 (1956) 463-466.

[21] D.N. Boccaccini, M. Cannio, M. Romagnoli, P. Veronesi, C. Leonelli, A.R. Boccaccini, The pO-index and R ratio gap methods for the assessment of corrosion risk in refractory materials in contact with glass melts, J. Am. Ceram. Soc. (2010). doi:10.1111/j.1551-2916.2010.03606.x.

[22] D.N. Boccaccini, M. Cannio, T.D. Volkov-Husoviæ, I. Dlouhy, M. Romagnoli, P. Veronesi, C. Leonelli, Assessment of viscoelastic crack bridging toughening in refractory materials, J. Eur. Ceram. Soc. (2008). doi:10.1016/j.jeurceramsoc.2008.01.021.

[23] D. Gardini, M. Blosi, C. Zanelli, M. Dondi, Ceramic Ink-Jet Printing for Digital Decoration: Physical Constraints for Ink Design, J. Nanosci. Nanotechnol. (2015). doi:10.1166/jnn.2015.9857.